LETTER • OPEN ACCESS

Methane emissions from rice cultivation in West Africa and compensation options from nature reserve forests

To cite this article: Samuel Guug *et al* 2025 *Environ. Res. Lett.* **20** 044050

IOP Publishing Environ. Res. Lett. 20 (2025) 044050 https://doi.org/10.1088/1748-9326/adc28c

ENVIRONMENTAL RESEARCH
LETTERS

RECEIVED
20 December 2024

REVISED
24 February 2025

ACCEPTED FOR PUBLICATION
19 March 2025

PUBLISHED
4 April 2025

LETTER

Methane emissions from rice cultivation in West Africa and compensation options from nature reserve forests

Samuel Guug[1,2,4,*], Souleymane Sy[3], Emmanuel Quansah[2], Jan Bliefernicht[3], Frank Neidl[4], Rainer Steinbrecher[4], Michael Ayamba[1], Alex Frempong[2], Patrick Davies[2], Ines Spangenberg[3,4], Francis E Oussou[5], Belko Aziz Diallo[1], Seyni Salack[1], Kwame Hackman[1], Leonard K Amekudzi[2], Kehinde Ogunjobi[1] and Harald Kunstmann[4,5,6]

[1] West African Science Service Centre on Climate Change and Adapted Land Use, WASCAL Competence Centre, Ouagadougou, Burkina Faso
[2] Department of Meteorology and Climate Science, Kwame Nkrumah University of Science and Technology, Kumasi, Ghana
[3] Institute of Geography, University of Augsburg, Augsburg, Germany
[4] Institute for Meteorology and Climate Research, Karlsruhe Institute of Technology, Campus Alpin, Garmisch-Partenkirchen, Germany
[5] The Federal University of Technology, Akure, Nigeria
[6] Center for Climate Resilience, University of Augsburg, Augsburg, Germany
[*] Author to whom any correspondence should be addressed.

E-mail: guug.s@wascal.org and harald.kunstmann@kit.edu

Keywords: methane, paddy rice, forest, greenhouse gas, agriculture, land-based mitigation, West Africa

Supplementary material for this article is available online

Abstract

Methane (CH_4) is a major and potent greenhouse gas (GHG), and its emissions from agricultural activities, particularly rice cultivation, are a significant concern for climate change. Due to the high demand for food security, driven by rapid population growth and national initiatives to reduce dependency on rice imports, rice cultivation is intensified in West Africa. However, its contribution to atmospheric CH_4 remains largely unknown. Here, for the first time, cutting-edge eddy covariance tower measurements were conducted parallelly in a rice field (Janga) and a reserve forest (Mole National Park), both located in the Guinea savanna region of West Africa. Using CH_4 measurement data from June to October 2023 (rice cultivation period), the dynamic interplay between methane emissions from rice cultivation and its potential mitigation through forest methane uptake was assessed. Our results show that the rice field acted as a net source of CH_4 at a rate of 2037 $mgCH_4m^{-2}$, whereas the most intense flooded period (August) accounted for 70% of the total emissions. On the other hand, the forest reserve acted as a sink, with a net uptake of -560 $mgCH_4m^{-2}$, and the highest uptake observed in October. Accounting for the global warming potential (GWP) of CH_4 over a 20 year period, the forest had a wet season negative GWP of -47.04 gCO_2eq, while the rice field emitted CH_4 of 171.36 gCO_2eq. This implies that under similar conditions during the measurement campaigns, the forest per square area needs approximately a factor of $\sim$4 to balance the positive radiative effect per square area of rice cultivated. This work emphasizes the need to integrate forests to compensate for methane released by rice cultivation in the semi-arid West African savannah region.

1. Introduction

West Africa has experienced a rapid population increase (Akintunde *et al* 2013), and it is projected to contribute to global population growth in the coming years significantly (Foley 2011, Van Bavel 2013). It will likely account for over half of the world's population growth by 2050 (Van Bavel 2013). The consequences of this population growth have exerted considerable pressure on the environment (Weber and Sciubba 2019), leading to intensive anthropogenically land-use changes and agricultural intensification (Sy *et al* 2017, Bliefernicht *et al* 2018, Potapov *et al* 2022, Sy *et al* 2024). Consequently, rice cultivation is being intensified in West Africa, mainly driven by the high demand for food security and national initiatives to reduce dependency on rice imports in the future (Chen *et al* 2024, Yuan *et al* 2024).

Rice is one of the major cereal crops globally, consumed daily by half the world's population, leading to increasing demand (Fahad *et al* 2018, Bin Rahman and Zhang 2023). This is especially true in West Africa, where a significant upward shift in rice consumption has been observed over the last ten years (Yuan *et al* 2024). This shift has resulted in a nearly ninefold increase in rice production between 1961 and 2019 (Bin Rahman and Zhang 2023). Given the rapid population growth and the need for rice self-sufficiency, the demand for rice in Africa, particularly in sub-Saharan Africa, is expected to double by 2050 (Yuan *et al* 2024).

Among the various atmospheric methane (CH_4) sources, rice paddy fields are considered a significant contributor (Zhang *et al* 2020, Nikolaisen *et al* 2023a). Methane emissions from rice fields, including irrigated, rain-fed lowland, and flood-prone fields, account for approximately 10% to 18% of all agricultural CH_4 emissions globally (IPCC 2014, FAO 2021) and 19% to 33% of current global terrestrial CH_4 emissions (Saunois *et al* 2020). In flooded paddy fields, methane is produced by the anaerobic breakdown of organic molecules. Flooding cuts off the oxygen supply to the rhizosphere, creating an anaerobic environment. This anaerobic decomposition of soil organic matter generates methane gas, which is released into the atmosphere through diffusion, ebullition, and the aerenchyma of plant roots and stems (Rahman and Yamamoto 2020, Heredia *et al* 2022).

In the context of global agreements to keep warming below 2 °C and strive to stay within 1.5 °C above pre-industrial levels, as adopted by many countries during the Paris COP21 Agreement (IPCC 2018), stringent climate change mitigation measures can heavily impact the agriculture sector (van Loon *et al* 2019). These measures pose challenges since sustainable development goals emphasize balancing climate change mitigation with achieving food security (United Nations 2016). However, there is considerable debate that prioritizing climate mitigation over food security, especially given the current population surge, may have a more detrimental impact than climate change. For instance, if climate mitigation measures lead to decreased agricultural productivity or increased food prices, this could exacerbate food insecurity, particularly in regions with high population growth rates, such as West Africa. Forest has been proposed as a crucial solution for sequestering atmospheric CH_4, significantly influencing the global CH_4 budget (Ni and Groffman 2018, Feng *et al* 2022). While some studies suggest that the methane sink capacity of forest soils has increased in recent decades (e.g. Yu *et al* 2017), there is still considerable disagreement among studies regarding the role of forest soils in methane dynamics. For example, (O'Connell *et al* (2018) showed that forest soils may become larger sinks or even sources of CH_4 depending on changes in soil conditions due to drought, flooding, warming, natural disturbances, and forest management. Furthermore, Frankenberg *et al* (2005) suggested that forest soils could be significant sources of CH_4 depending on the forest ecosystem, thereby challenging the traditional view that forests consistently act as sinks for atmospheric CH_4. However, little is known about how soil CH_4 sinks or sources respond to changing environmental conditions (Feng *et al* 2022). This is especially true in the semi-arid West African savannah region, where data are scarce, and the lack of continuous CH_4 *in situ* measurements limits the available evidence (Ni and Groffman 2018, Feng *et al* 2022). Additionally, although measurements of CH_4 flux have been conducted in forests worldwide, most studies have focused on mid-latitude regions and are limited to tropical forests (Barthel *et al* 2022).

Here, for the first time, we investigate the dynamic interplay between methane emissions from rain-fed rice cultivation and their potential mitigation through forest methane uptake in the semi-arid West African savannah region. Using advanced micro-meteorological measurement equipment and eddy covariance (EC) flux towers, one-year measurements of soil methane fluxes were conducted simultaneously in a paddy rice field in Janga and a protected forest reserve in Mole National Park (both located in northern Ghana) (see Methods). Notably, this study enhances our understanding of how protected forest reserves can effectively mitigate CH_4 emissions from rain-fed rice agriculture in this region. This study addresses two main scientific questions: (i) to what extent can forest in the semi-arid West African savannah region sequester methane emissions from rice cultivation? (ii) What underlying factors control methane dynamics in forest ecosystems and rice agriculture in the semi-arid West African savannah region?

2. Materials and methods

2.1. Study area and field sites

The study area (see figure 1(a)) is part of a large observatory established over the last decade, initially focused on CO_2 and H_2O measurements (Quansah *et al* 2015, Bliefernicht *et al* 2018, Berger *et al* 2019) by a German-African research initiative in the West Africa's Sudanian savanna belt. This network was extended by establishing two new EC stations: one in a rice field (hereafter 'Janga', dominated by floodplains) and another in a forest reserve (hereafter 'Mole') to include CH_4 measurements with the aim to compare CH_4 emissions/uptake in two ecosystems with contrasting land-use and land management practices in northern Ghana (see figure 1(b).c vs figure 1(f).g). The local climate at both sites is influenced by the

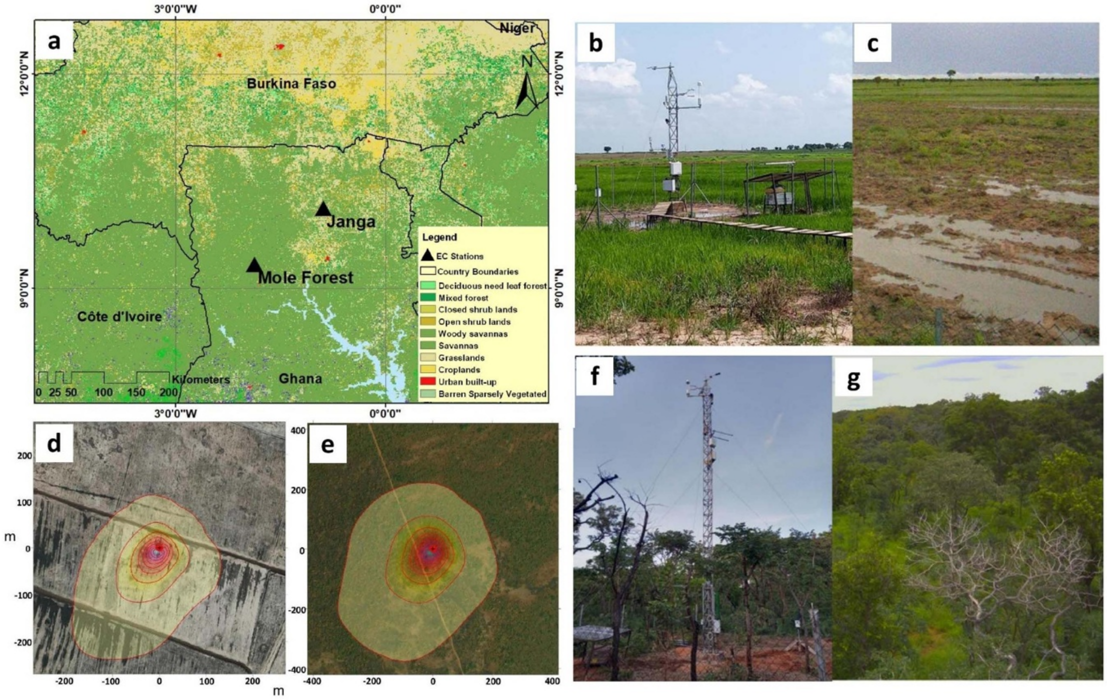

Figure 1. Dominant land cover fractions over the study area, derived from the MODIS land cover map based on the International Geosphere-Biosphere Programme (IGBP) 21-category classification (Sulla-Menashe *et al* 2019). The most prominent land use types are cropland and grassland (in yellow/orange), with savannah (in green) predominantly in north of Ghana. (b) The Janga rice field and EC tower, with an image of a flooded field (c) and its footprint area (d). (f) The Mole forest site and EC tower, with an image of the vegetation cover (g) and its footprint area (e). The flooded field and vegetation cover images (c) and (g) were taken with a CCFC field camera (Campbell Scientific Inc., Logan, UT). Footprint areas were calculated using the Kljun FFP online tool (Kljun *et al* 2015).

West African monsoon (Nicholson 2013). It is characterized by two distinct seasons: a wet season from May to October and a dry season from November to March (Nicholson 2013). Annual rainfall ranges from 900 to 1100 mm and is mainly driven by mesoscale convective systems (Nicholson 2013). These systems result in highly variable spatio-temporal rainfall patterns, which pose significant challenges to rain-fed agricultural activities. Temperatures range from 22 °C to 34 °C, with maximum temperatures of up to 40 °C occurring in March/April (Nyadzi *et al* 2021, Dakwa 2018).

Soils within the Janga rice field are predominantly Plinthic Ferralsols (groundwater laterites) and EutricNitosols (savannah ochrosols), with varying soil textures from fine sands, loam, and heavy clays (Addai 2016). The catchment is characterized by broad valleys and extensive floodplains with limited drainage (Abdul-Ganiyu *et al* 2011). Rice and maize are the major crops grown during the rainy season, mainly along the floodplains. The Mole Forest was officially designated in 1958 as a national park (Awuah 2017). The park's management is under the wildlife division of the Ghana Forestry Commission, and it is classified as a Category II National Park according to the International Union for Conservation of Nature (IUCN) classification of protected areas (Cole Burton *et al* 2011). The dominant vegetation is open savanna woodland and other smaller plant communities, such as swamps and floodplains, with a grass layer that can grow up to 3 m tall in the rainy season (Schmitt and Adu-Nsiah 1993). According to Bowell and Ansah (1994), the forest soil characteristics consist of a combination of Ferrosol with an abundance of free iron and well-defined structural Nitisol, demonstrating effective drainage properties.

2.2. Site instrumentation

Measurement campaigns started in June 2022 with the setting up of EC towers at a rice field (figure 1(b)) in Janga (Long: −0.8838, Lat:10.1299) and in May 2023 at a reserve forest (figure 1(f)) in the Mole National Park (Long: −1.8688, Lat: 9.3388). CH_4 turbulent fluxes were measured at 10 Hz (12 m height) in the forest and 20 Hz (3.4 m height) in the rice field using LI-7700 laser spectroscopy gas analyzers (LI-COR Inc., Lincoln, USA) and an IRGASON, an integrated infrared gas analyzer, and sonic anemometer (Campbell Scientific Inc., Logan, UT). In addition, meteorological data such as air temperature, relative humidity, solar radiation, and precipitation were measured and stored in 30 min resolution. We also measured soil water content (SWC) and temperature at 3, 10, and 35 cm and three ground heat flux plates placed at 8 cm to measure ground heat energy. All data variables were logged in CR6 data recording loggers with an external 16 GB storage capacity (Campbell Scientific). Field cameras were installed at each site and focused on the mean wind direction to monitor the field management and vegetation cover (e.g. figures 1(c) and (g)). In addition to our regular site visits for maintenance, the automated cleaning of the CH_4 laser sensor (LI-7700) was implemented, which routinely washed the laser mirror every three hours when the signal strength (RSSI) drops below 50%. Field computers were permanently installed at each site for data storage, pre-processing, and transmission.

2.3. Data processing

The CH_4 turbulent data were processed and quality controlled into half-hourly fluxes using the Turbulence Knight (TK3) statistical routine tool (Mauder and Foken 2006, Mauder *et al* 2008). We performed plausibility tests on the turbulent data with consistency limits and excluded physical or electronic not possible values. A signal strength (RSSI) of 10% was set as a threshold for the CH_4, similar to Staudhammer *et al* (2022), where we excluded values below this threshold. TK3 then calculated the averages, variances, and covariances of the raw data and then averaged 30 min and 5 min intervals with an automatic lag correction by maximizing covariances to account for delays of the time series caused by different sensors. A stationary test (Foken and Wichura 1996) was performed to compare the 30 min covariances with those for 5 min averaging time where data that deviates >30% is set to flag 1 and >100% to flag 2. All these steps are performed taking into consideration the EC theory. The coordinate rotation (Kaimal and Finnigan 1994) was performed considering the wind fields at each site. The data was screened for spikes, followed by detrending, and the time delay between the turbulent vertical and the scalar wind measurements of the different sensors by cross correlation analysis for each averaging interval (Mauder *et al* 2013, Vitale *et al* 2020). These were finally followed by the Webb, Pearman, and Leuning correction for density fluctuations of ambient air (Schotanus *et al* 1983, Liebethal and Foken 2003, Jentzsch *et al* 2021). The CH_4 flux was calculated as:

$$F_{CH_4} = \overline{w' \rho c'} \tag{1}$$

where $\rho\dot{c}$ the instantaneous fluctuation of the CH_4 density w' is the instantaneous fluctuation between the vertical wind velocity and the overbar denotes a time average (Burba *et al* 2013). The relative random flux and noise errors were calculated on the final processed fluxes following (Mauder *et al* 2013). We considered flagging according to Mauder and Foken (2006), where high-quality fluxes are flagged '0', intermediate-quality fluxes are flagged '1′ (suitable for general analysis such as annual and seasonal budgets), and poor-quality fluxes are flagged '2′ (usually discarded).

2.4. CH_4 flux drivers selection and gap-filling

We performed gap-filling to ensure a continuous time series for calculating CH_4 budgets (see figures S2 and S3). These data gaps occurred due to rain events, instrument signal quality thresholds, and filtering during data quality control, accounting for less than 30% of missing data points at both sites. Even though no single standardized approach has been developed for filling data gaps in CH_4 fluxes, we considered a machine learning approach random forest (RF) in this study (Kim *et al* 2020, Irvin *et al* 2021). Several biophysical environmental predictors were pre-selected following previous studies (e.g. Kim *et al* 2020, Irvin *et al* 2021, Lucas-Moffat *et al* 2022, Zhu *et al* 2023) on CH_4 fluxes from wetlands and forest ecosystems. To identify the most important predictors, we considered a machine learning model—RF, an ensemble decision tree built independently from bootstrapped data samples (Breiman 2001). RF has been tested and used for CH_4 flux driver selection and gap filling at several sites (Kim *et al* 2020), which have proven robust (Irvin *et al* 2021, Lucas-Moffat *et al* 2022). We used the scikit-learn library (Pedregosa *et al* 2011) to implement the RF learning regressor models and the SciPy package for statistical testing, both in Python. A supervised learning estimator was used to generate 100 decision trees randomly. We assessed the correlation between the target (CH_4) and the pre-selected predictors was performed using 70% of the quality-controlled data for training and 30% for testing. Each predictor variable was assigned a feature importance score representing their relative influence on methane flux prediction (James *et al* 2013). The predictor variables with a feature important score < 0.05 were eliminated (Maier *et al* 2022) as input predictor variables for the gap-filling process. For consistency, the gap-filled dataset was used in all analyses presented in this study.

Finally, the same process was repeated, considering the important predictors identified as input variables for the gap-filling of the CH_4 fluxes, considering 1000 randomly generated (with bootstrapped with replacement) decision trees. We calculated the R^2 score on the bootstrapped (original) and the predicted to ascertain how well the observed methane flux matched the predicted values from the models. The relationship between the gap-filled CH_4 fluxes and each driver was further analyzed by binning data at fixed interval increments of the independent variable corresponding to CH4 (Emerson *et al* 2021) and averaging values within defined intervals. We applied a simple Polynomial Regression with a quadratic fit to compare their explanatory power with a 95% confidence interval.

2.5. Global warming potential (GWP)

The impact of the concentration of CH_4 for the two sites was assessed by evaluating their radiative effects (Ali *et al* 2013). Specifically, it quantified the net CH_4 uptake of the forest ecosystem and its potential to mitigate the warming effect of CH_4 emissions from rice cultivation. This was done using CO_2 as the reference gas for calculating GWP (see Rabbi and Kovács 2024). To do this, the CH_4 flux balances from each site were converted to CO_2 equivalents, following methods described in previous studies (Ramaswamy *et al* 2001, Frolking *et al* 2004, Boucher *et al* 2009). The GWP of CH_4 was calculated as follows:

$$\mathrm{GWP}^{t}_{\mathrm{CH_4}} = \frac{\int_0^t A_{\mathrm{CH_4}}\left[r_{\mathrm{CH_4}}(t)\right]\mathrm{d}t}{\int_0^t A_{\mathrm{CO_2}}\left[r_{\mathrm{CO_2}}(t)\right]\mathrm{d}t} \quad (2)$$

where A is the radiative forcing per unit mass of CH_4 or CO_2, and $r(t)$ is the response function or decay in the concentration of CH_4 or CO_2 at time horizon (t), typically 20, 100 years (see Rabbi and Kovács 2024). Based on the IPCC Fifth Assessment Report (IPCC 2014), the updated values of the 20- and 100 year GWP factors for CH_4 flux in CO_2 equivalents (CO_2eq) are 84 and 27, respectively.

3. Results

3.1. Environmental variables

The environmental parameters at both sites during the study period (June to October) are illustrated in figure 2. On average, air temperature was slightly higher in the rice field (28.9 °C) than in the forest site (27.6 °C) (figure 2(e)). The forest site received more incoming solar radiation (SW_IN) during the daytime than the rice field (figure 2(a)). As expected, latent (LE), and sensible (H) heat fluxes peaked higher during the daytime in the forest site than in the rice field (figures 2(b) and (c)) due to the forest canopy capacity to absorb more solar energy (lower albedo) during daytime for photosynthetic activities and leading to high evapotranspiration. Furthermore, on average, the rice field (open land) wind speed was 2 times higher (2.48 m s^{-1}) than the forest site with 1.24 m s^{-1}. Winds from the southeast and southwest at the rice field were dominant and likely contributed more to the CH_4 fluxes (figure 2(g)), as seen in the footprint analysis (figure 1(d)). In contrast, winds from the forest site were distributed across the Northwest, Southeast, and Southwest directions (figure 2(h)) which resulted in the distributions of the CH_4 fluxes across all these directions as also observed in the footprint analysis (figure 1(e)). Regarding the precipitation, the rice field and forest sites had a total rainfall of 613 and 670 mm during the rainy season respectively, where both sites recorded the highest rainfall in July (figure 2(f)). Overall, both sites exhibited comparable local climatic characteristics, with the forest site experiencing slightly cooler, wetter conditions (lower temperature and higher humidity) than the rice field.

3.2. Dynamics of CH_4 fluxes

CH_4 fluxes showed considerable variability across both sites throughout the study period (see figure 3). Additionally, obvious diurnal variations were observed at the two sites, with peak positive and negative values occurring at different times of the day (figure 4) likely driven by various underlying physical mechanisms, including meteorological and biological factors (see figure 5). Over the rice field, as expected, SWC at 5 cm vapor pressure deficit and soil temperature (Tsoil) at 10 cm remained the predominant factors controlling CH_4 dynamics (with R^2 values up to 0.59; $p < 0.05$) (see figure 5). Significant variations were observed across different growth stages (figures 3(c) and (e)), with an average CH_4 flux of 9.70 ± 22.34 nmol m^{-2} h^{-1}, ranging from −71.85 to 169.44 nmol m^{-2} h^{-1}. During the start of the rainy season, the highest CH_4 flux recorded in June was 40.47 nmol m^{-2} h^{-1}. Subsequently, after the field was prepared (plowed and harrowed on July 22), followed by substantial rain events, CH_4 increased sharply, resulting in substantial-high positive fluxes during August, with a peak hourly flux reaching 169.44 nmol m^{-2} h^{-1}. However, notable negative CH_4 fluxes were also observed during the maturing and ripening stages (September and October), with CH_4 flux reaching −71.85 nmol m^{-2} h^{-1}. The peak diurnal CH_4 fluxes for the first three months (June–August) occurred between 08:00 and 15:00 UTC (figure 4(a)). June and July had diurnal peak fluxes of 11.43 ± 11.09 nmol m^{-2} h^{-1} at 12:00 UTC and 9.65 ± 29.19 nmol m^{-2} h^{-1} at 09:00 UTC, respectively, while August showed the highest diurnal peak of the season with 58.68 ± 40.68 nmol m^{-2} h^{-1} which occurred at noon. Fluxes in September and October were notably lower during the day but peaked during nighttime at 19:00 UTC (14.66 ± 32.39 nmol m^{-2} h^{-1}) and 20:00 UTC (6.38 ± 8.98 nmol m^{-2} h^{-1}), respectively.

In contrast, at the forest site, the dominant factors influencing CH_4 dynamics were vapor pressure deficit, latent heat flux, ecosystem respiration, and soil temperature (figure 5(b)). These factors showed statistically significant relationships (with R^2 up to 0.65; $p < 0.05$). Furthermore, the forest site demonstrated a gradual variation in CH_4 fluxes (figure 3(f)), with

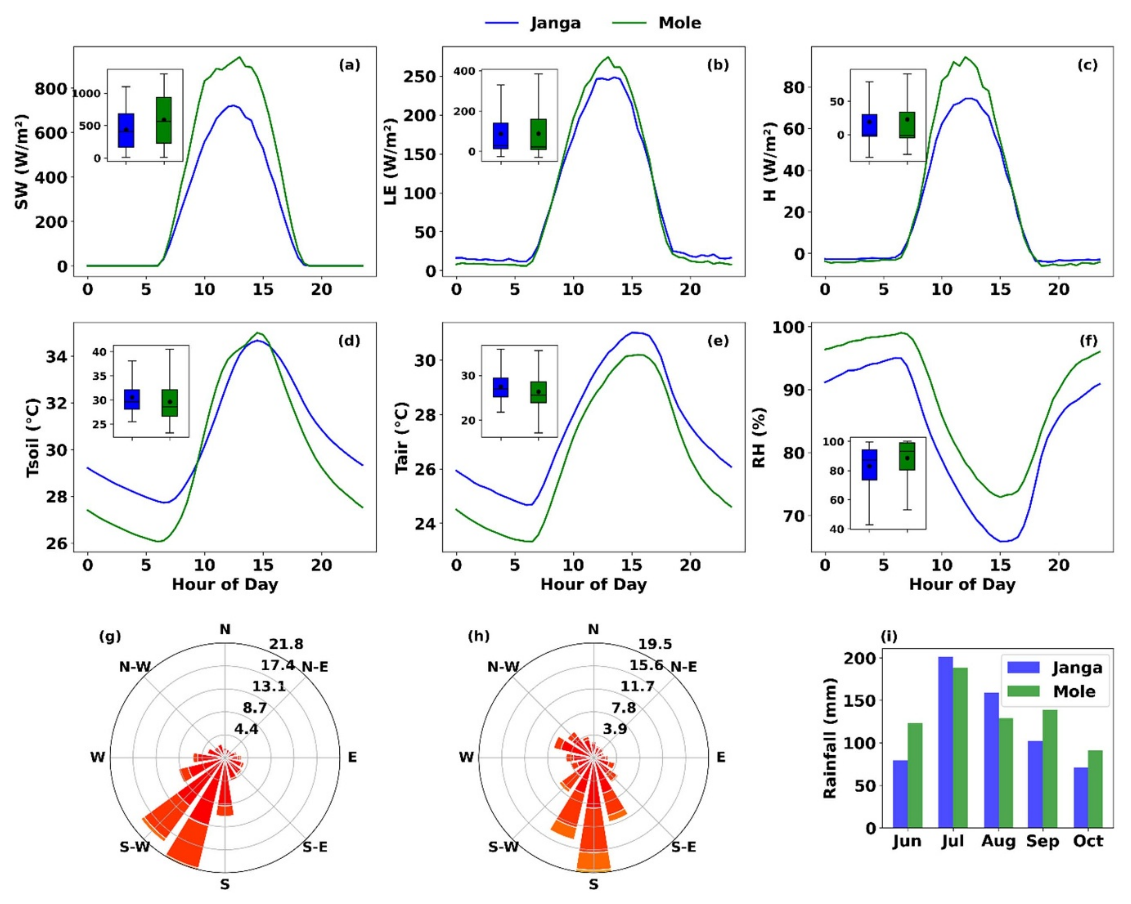

Figure 2. Temporal variation of environmental variables including the diurnals (a) solar radiation, (b) latent heat, (c) sensible heat, (d) soil temperature (5 cm), (e) air temperature, and (f) relative humidity (RH) at the paddy rice field (blue) and the forest reserve (green). Boxplots show the median, upper, and lower quartiles and the black dot represents the seasonal averages. Windrose of the mean wind direction at the rice field (g), the forest (h), and monthly rainfall totals (i).

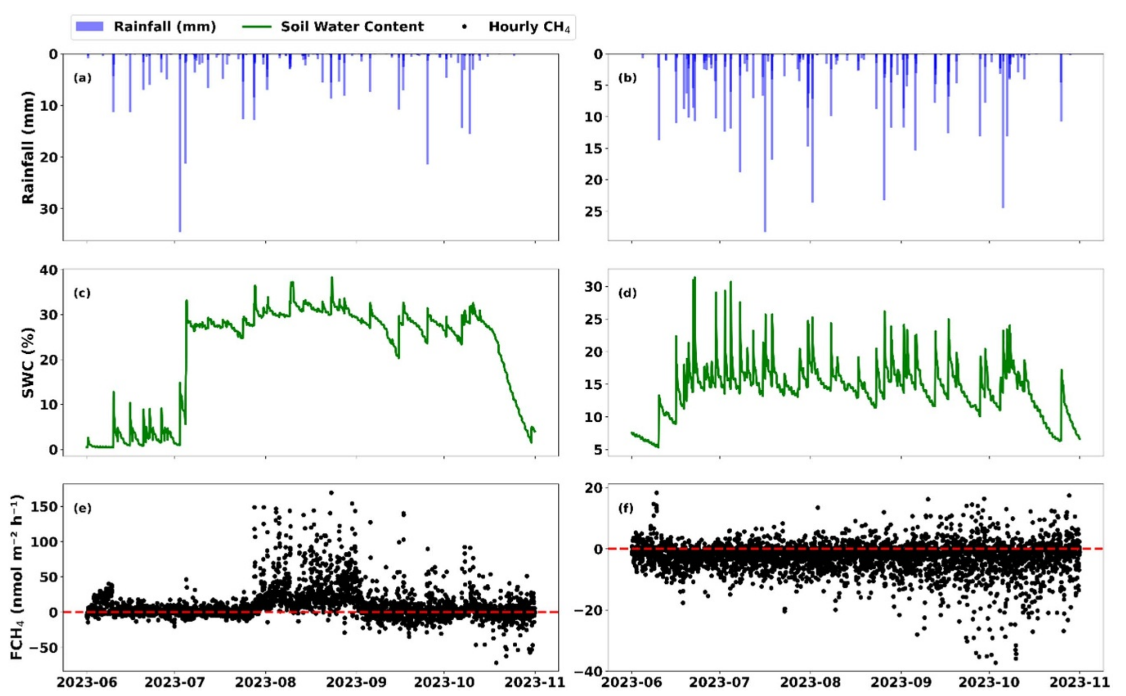

Figure 3. Daily variations in rainfall (a), (b) and soil water content (c), (d), along with hourly CH_4 fluxes represented by black dots (e), (f), are shown for the paddy rice field (left panels) and the forest reserve (right panels).

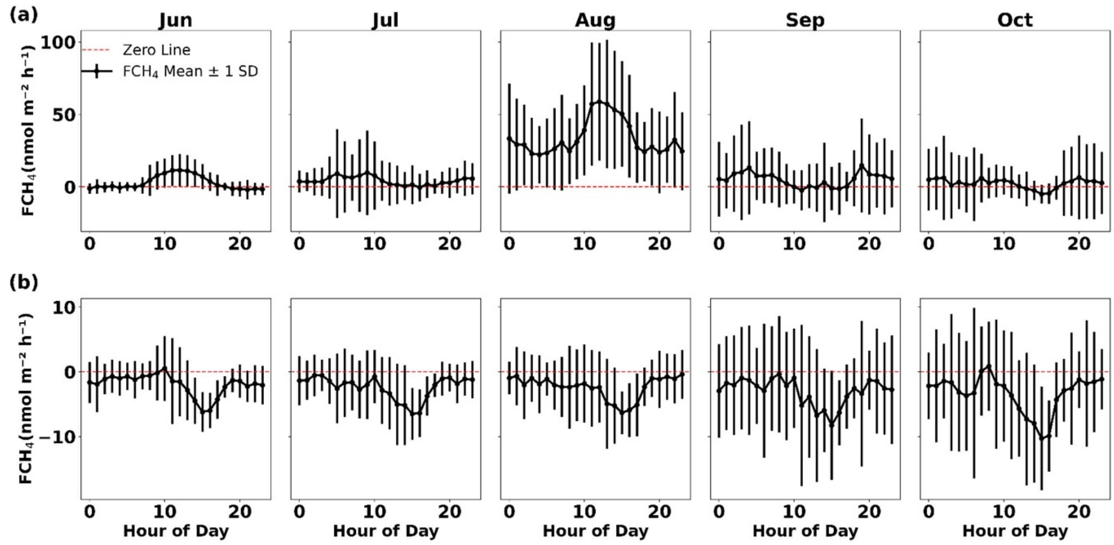

Figure 4. Average diurnal of CH_4 binned by time of day for each month during the rainy season for the paddy rice field (a) and the forest reserve (b).

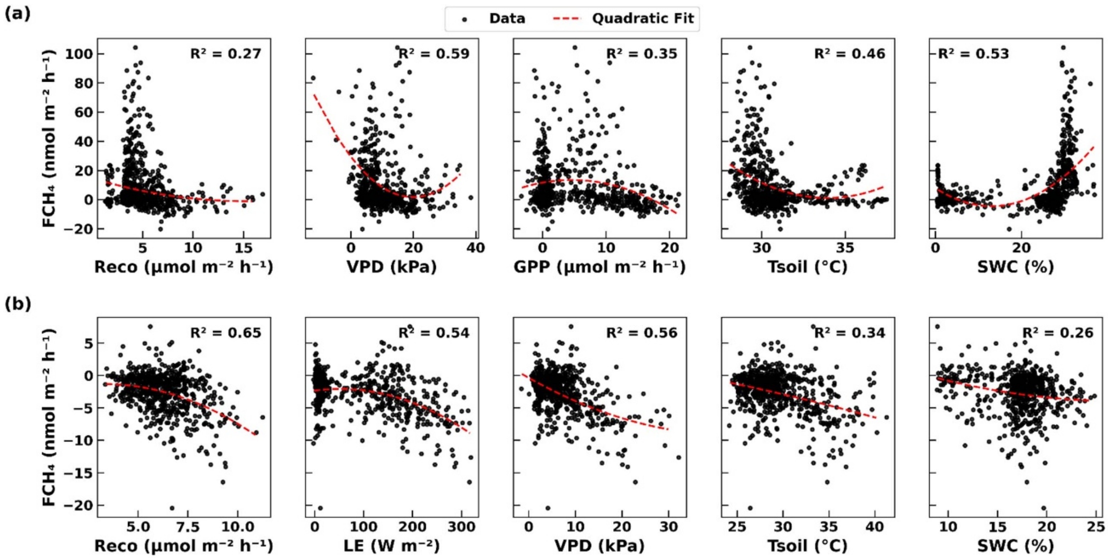

Figure 5. Contribution of each potential explanatory covariate factor predicting CH_4 fluxes for both the rice field (a) and forest site (b). SWC, Tsoil, VPD, LE, Reco, and GPP represent the soil water content at 5 cm, soil temperature, vapor pressure deficit, latent heat flux, ecosystem respiration, and gross primary production, respectively. The data were binned by a fixed interval increment of the CH_4, with values averaged within these defined intervals. A polynomial regression was applied to the binning for trend estimation and Pearson correlation for statistical relationships.

an average of -2.64 ± 5.10 nmol m^{-2} h^{-1}, ranging from -37.26 to 18.34 nmol m^{-2} h^{-1}. During the early part of the rainy season (June), CH_4 fluxes varied from -17.67 to 18.34 nmol m^{-2} h^{-1}, and afterward, negative fluxes were frequently observed in September (-35.29 to 16.34 nmol m^{-2} h^{-1}) and October (-37.26 to 17.45 nmol m^{-2} h^{-1}). There were more consistent negative CH_4 fluxes throughout the diurnal cycles (figure 4(b)), with all peaks observed at around 15:00 UTC. The highest diurnal negative flux of -10.30 ± 7.99 nmol m^{-2} h^{-1}, was recorded in October, while August had a diurnal peak of -8.26 ± 8.45 nmol m^{-2} h^{-1}. Consistent upward increases in CH_4 fluxes in the early morning (between 06:00 and 10:00 UTC) were observed due to the night-time storage of CH_4 fluxes.

3.3. Daily and seasonal CH_4 balance

The seasonal CH_4 balance is presented in figure 6, where negative CH_4 values denote the ecosystem's uptake (sink), and positive indicates emission (source) into the environment. The rice field (figure 6(a)) exhibited more frequent daily CH_4 emissions than uptake, with daily cumulative values ranging from -12.36 to 86.78 mgCH_4 m^{-2} d^{-1}. During the initial stage of the cultivation, emissions were low, with total net emissions in June and July at 117.06 and 178.04 $mgCH_4\ m^{-2}\ month^{-1}$, respectively. The highest CH_4 emission was recorded in August, reaching a total of 1440.97 $mgCH_4\ m^{-2}month^{-1}$. Consequently, emissions dropped to a net cumulative of 206.75 mg $CH_4\ m^{-2}month^{-1}$ in September and to 94.26 $mgCH_4\ m^{-2}\ month^{-1}$ in October. However, despite this decline, the rice field acted as a net CH_4 source throughout the cultivation period, with a total cumulative emission value reaching 2037.09 $mgCH_4\ m^{-2}$. Notably, August, characterized by extended periods of flooding, accounted for 70% of these emissions. In contrast, the forest area (figure 6(b)) demonstrated more frequent daily CH_4 uptake than emissions, with daily cumulative values ranging from −13.12 to 1.83 $mgCH_4\ m^{-2}\ d^{-1}$. In other words, the forest was consistently a CH_4 sink during the study period, showing minimal variation in the monthly uptakes. During the early part of the season, cumulative CH_4 uptake was −81.99 $mgCH_4\,m^{-2}month^{-1}$ in June. Uptake gradually increased throughout the season, peaking in October at −145.17 $mgCH_4\ m^{-2}month^{-1}$, resulting in a total net seasonal uptake of −560.23 $mgCH_4\,m^{-2}$.

In terms of GWP, table 1 shows that CH_4 emissions from the rice field, totaling 2.04 g $CH_4\ m^{-2}$ result in a positive radiative forcing equivalent to 171.11 g CO_2-eq over a 20 year GWP period. In contrast, the forest had a net CH_4 uptake of −0.56 g $CH_4\ m^{-2}$, corresponding to a negative radiative forcing of −47.04 g CO_2-eq over the same period. To offset the positive radiative effect of CH_4 emissions from an equivalent area of rice fields would require about four times the area of forest per m^2.

4. Discussion

This study represents the first investigation of CH_4 dynamics between two distinct ecosystems (a rice field and a forest reserve), with contrasting land use and management practices and their seasonal CH_4 balance in the semi-arid savanna region of West Africa. Although numerous studies have examined CH_4 emissions from wetland and forest ecosystems globally using various approaches, including remote sensing, modeling, EC, and chamber measurements (e.g. Peltola *et al* 2019, Wang *et al* 2021, Saderne *et al* 2023, Ouyang *et al* 2023), the majority of these studies have focused on mid-latitude regions and/or have been limited to tropical forests (Barthel *et al* 2022). Additionally, studies focusing on African ecosystems are relatively scarce and have predominantly relied on static chamber methods (e.g. Otter and Scholes 2000, Gasore 2007, Wanyama *et al* 2019, Castaldi *et al* 2020, Laris *et al* 2021).

Our study shows significant variations in CH_4 emissions during the rice growing season, mainly due to variations in hydrological conditions. Specifically, increased CH_4 emissions were observed on days following precipitation events, increasing SWC and leading to prolonged field flooding (figure 3(c)), consistent with previous studies (e.g. Alberto *et al* 2014). The intense flooding, and early stages of rice plant growth, created anaerobic conditions conducive to CH_4 production through methanogenesis, resulting in significant emissions in August (figure 6). During the maturation and ripening stages, the development of intercellular aerenchyma in rice plants likely facilitated oxygen transport between the atmosphere and the anaerobic zone (Lou *et al* 2008, Meijide *et al* 2011, Swain *et al* 2018). Furthermore, reduced field inundation contributed to a sharp decrease in CH_4 emissions in September and October, consistent with the observations of Wang *et al* (2017). Furthermore, the reported CH_4 fluxes from this study, ranging from −4.15 to 9.78 $mgCH_4\ m^{-2}\ h^{-1}$ (−12.36 to 86.78 $mgCH_4\ m^{-2}\ d^{-1}$), were comparable to values observed in previous studies based on paddy rice fields (Alberto *et al* 2014, Haque *et al* 2016, Martínez-Eixarch *et al* 2021), as well daily emissions rates (0.24 to 0.38 $kgCH_4$-C $ha^{-1}\ d^{-1}$ or 32 to 50.1 $gCH_4\ m^{-2}\ d^{-1}$) in Ghana by Nikolaisen *et al* (2023b). The total amount of CH_4 emitted from June to October (2.01 $gCH_4\ m^{-2}$), was close to reported seasonal fluxes of 3.26 $gCH_4\ m^{-2}$ (Alberto *et al* 2014), 2.1 to 2,9 $gCH_4\ m^{-2}$, (Hatala *et al* 2012) and 5.01 $gCH_4\ m^{-2}$ (Reba *et al* 2020). However, our study cumulated flux value was far lower than values of 27.9 gC m^{-2} or 37.2 $gCH_4\,m^{-2}$ (Meijide *et al* 2011) and 36.05 $gCH_4\ m^{-2}$ (Maboni *et al* 2021) for continuous flooded rice fields. The relatively lower cumulative flux observed in our study could be attributed to the intermittent rainfall events which created multiple drying cycles. This may have inhibited continuous CH_4 production while enhancing CH_4 oxidation by methanotrophs. Notably, periods of continuous flooding, particularly in July and August, accounted for more than 75% of the cumulative emissions.

In the case of the forest reserve, CH_4 uptake increased slightly from June to July. However, CH_4 emissions remained at the same rate in August due to high SWC, which suppressed soil temperature and limited oxygen exchange. These conditions inhibited methanotrophic activity while promoting methanogenesis, consistent with findings from previous studies Wang *et al* (2021); Zhu *et al* (2021). As SWC decreased to an average of ∼15% in September and further to ∼12% in October (figure S1(a)) due to reduced rainfall and slightly elevated soil temperatures (figure S1(b)),

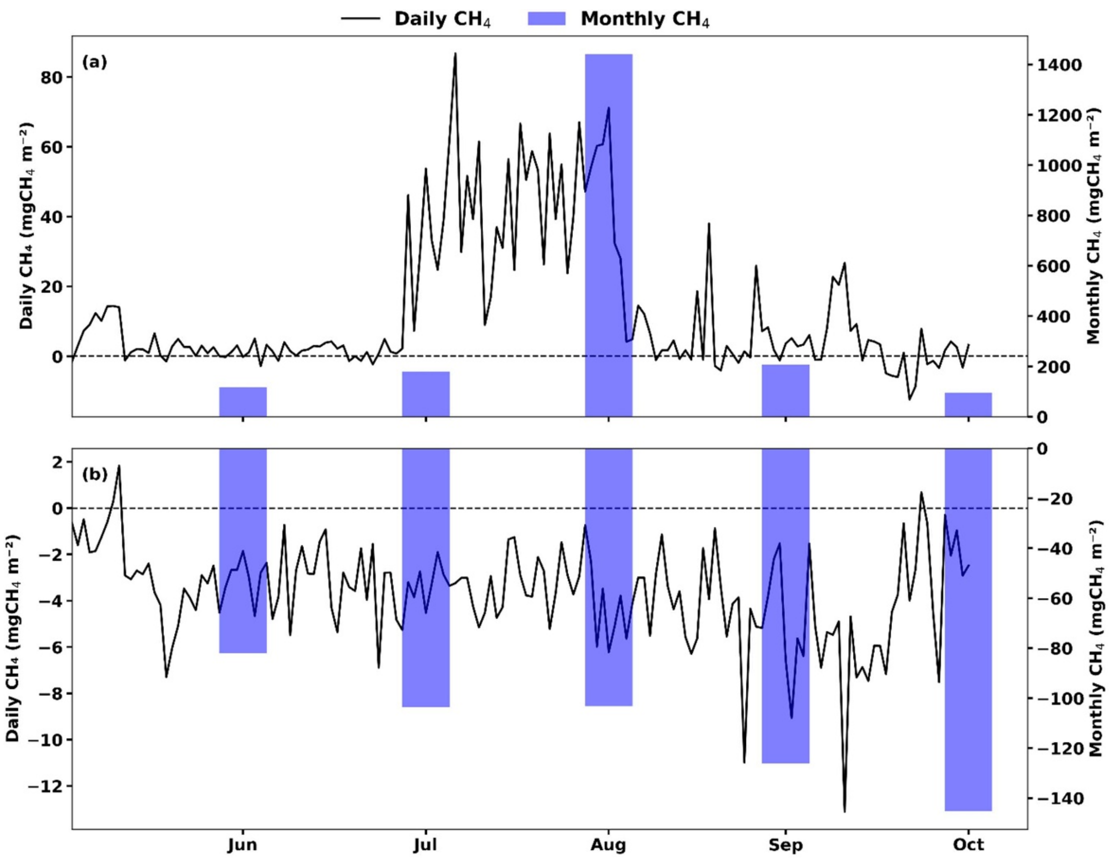

Figure 6. Daily cumulative (line) and monthly totals (bar) of CH_4 fluxes of the paddy rice field (a) and the forest reserve (b).

Table 1. Net radiative forcing of CH_4 expressed as CO_2 equivalent (gCO_2eq) using 20 and 100 year global warming potential (GWP) factors.

Month		June	July	August	September	October	Wet season (Total)
Rice field	CH_4 (gCH_4m^{-2})	0.12	0.18	1.44	0.21	0.09	2.04
	GWP_20 (gCO_2eq)	9.83	14.95	120.96	17.31	7.89	171.11
	GWP_100 (gCO_2eq)	3.27	4.98	40.32	5.79	2.63	57.04
Forest reserved	CH_4 (gCH_4m^{-2})	−0.08	−0.10	−0.10	−0.13	−0.14	−0.56
	GWP_20 (gCO_2eq)	−6.88	−8.74	−8.65	−10.58	−12.18	−47.04
	GWP_100 (gCO_2eq)	−2.30	−2.91	−2.88	−3.53	−4.06	−15.68

conditions became favorable for methanotrophic activity, thereby increasing CH_4 uptake. This result was expected, as methanotrophs are more sensitive to soil desiccation than methanogens (Megonigal and Guenther 2008), and elevated temperatures are known to accelerate their activity (Yvon-Durocher *et al* 2014, Knox *et al* 2021). In particular, vapor pressure deficit and latent heat flux, which regulate soil moisture and evaporation, respectively, emerged as key factors influencing CH_4 dynamics in the forest site (figure 5(b)). Our finding is also consistent with previous studies showing that upland forests function as CH_4 sinks (e.g. Zhao *et al* 2019, Castaldi *et al* 2020). The seasonal average CH_4 uptake value (-3.66 ± 2.09 mg CH_4 m^{-2} d^{-1}) observed in our study aligns with the range reported in other forest ecosystems. For example, Castaldi *et al* (2020) found that CH_4 uptake values ranged from -1.29 to -0.44 mg CH_4 m^{-2} d^{-1}, while Barthel *et al* (2022) reported similar findings in the Congo Basin using static chambers. Additionally, Wang *et al* (2021) observed CH_4 uptake ranging from -2 to -6 mg CH_4 m^{-2} d^{-1} in a subtropical forest during the rainy season (June to October). Differences in daily CH_4 dynamics across these studies can likely be attributed to variations in plant composition, soil characteristics, and microbial communities among forest ecosystems. Nevertheless, these findings reinforce our conclusion that the Mole forest (Guinea savanna) acts as a CH_4 sink during the rainy season, emphasizing the importance of environmental factors in regulating CH_4 fluxes.

Our findings also reveal a significantly strong positive CH_4 radiative forcing from the rice field at

Janga, highlighting the need for special and resilient mitigation options, especially considering its impact on global warming over a 20 year horizon. In other words, rainfed rice cultivation in paddy fields may be a strong net positive radiative forcing in the next decades, considering the self-sufficiency rice production policy in the African continent than perhaps previously recognized (Arouna *et al* 2021, Luo *et al* 2023). Although the Mole forest exhibited a relatively weak negative radiative forcing per unit area (-47.04 g CO_2-eq m^{-2}) compared to the positive radiative forcing of the rice field (171.11 g CO_2-eq m^{-2}), its extensive land area of about 4840 km^2 (Schmitt and Adu-Nsiah 1993), with a significant proportion of which consists of upland soils favorable for methane uptake, could represent a substantial CH_4 sink. This sink can potentially offset the radiative forcing produced by several hectares of rice cultivation under paddy conditions. These findings highlight the critical role of protected upland forests as climate-smart, nature-based solutions for mitigating CH_4 emissions. Moreover, this is in line with international policies that promote forest conservation as an effective strategy for carbon sequestration and greenhouse gas mitigation (van der Gaast *et al* 2018).

5. Conclusion

At the regional level, our results have important implications for climate change mitigation strategies and policy development. They highlight the importance of recognizing the capacity of forest areas as CH_4 sinks to offset its emissions from rice cultivation and their impact on regional and global climate change. Our study showed that the rice field was a continuous source of CH_4 throughout the cultivation period, with SWC and vapor pressure deficit identified as the main driver of these high emissions. Conversely, the forest area acted as a net CH_4 sink, with key influencing factors including ecosystem respiration, vapor pressure deficit, latent heat, and soil temperature. These results provide important insights into the dynamics, environmental controls, and seasonal balance of CH_4 emissions and uptake in contrasting ecosystems with different land use and land management practices. In other words, this study emphasized the critical need for exploring mitigation strategies to combat climate change, particularly through the measurement of CH_4 due to its high radiative forcing potential in the atmosphere.

Our continuous EC measurements of CH_4 fluxes, which integrate emissions from soil and atmosphere within a footprint area, provided a more comprehensive and representative dataset than conventional static chamber methods. It is worth noting that our results are based on observations from a single rainy season. However, long-term measurements, including other key greenhouse gases such as N_2O, are essential to capture the two contrasted ecosystems' full variability, dynamics, and overall carbon balance. Although our study focuses on rainfed rice cultivation, which accounts for about 70% of the total rice area harvested in sub-Saharan Africa—of which about 40% is classified as lowland rainfed without water control (Dossou-Yovo *et al* 2022, Saito *et al* 2023)—future research should include irrigated rice fields to assess their contribution to methane emissions relative to rainfed systems. In addition, further studies are needed to assess the impact of anthropogenic activities, such as fire events at the forest site, which could diminish its CH_4 uptake capacity. These findings demonstrated that forests could hold significant potential as climate-smart solutions for balancing ecosystem CH_4 emissions, particularly from rice cultivation, when protected from activities that compromise their CH_4 sink capacity. This highlights the dual benefits of integrating forest conservation with rice cultivation expansion as a viable land-based climate change mitigation strategy.

Data availability statement

The data that support the findings of this study are available from the corresponding authors upon reasonable request.

Acknowledgments

This research was funded by the German Federal Ministry of Education and Research (BMBF) through the West African Science Service Center on Climate Change and Adapted Land Use (WASCAL) and the Concerted Regional Modelling and Observation Assessment for Greenhouse Gas Emissions and Mitigation Options under Climate and Land Use Change in West Africa (CONCERT-West Africa; Grant No. 01LG2089A BMBF). The authors would like to thank the authorities of Mole National Park of the Forestry Commission and the landlord (Chief Ibrahim Johnson) of the Janga rice field for allowing the installation of the eddy covariance (EC) stations. The authors would also like to thank the two anonymous reviewers for their constructive comments, which helped improve the paper.

Conflict of interest

The authors declare no competing financial interests.

Contributions

Samuel Guug performed the analyses and drafted the first manuscript. Samuel Guug, Frank Neidl, Rainer Steinbrecher, Souleymane Sy, Alex Frempong, Ines Spangenberg, Patrick Davies, and Michael Ayamba set up the EC stations and performed calibrations and maintenance. Souleymane Sy, Emmanuel Quansah and Harald Kunstmann supervised the research. All authors contributed their expertise in developing the manuscript.

ORCID iDs

Samuel Guug https://orcid.org/0000-0002-2900-2179
Souleymane Sy https://orcid.org/0000-0001-8834-7620
Emmanuel Quansah https://orcid.org/0000-0002-3382-1775
Jan Bliefernicht https://orcid.org/0000-0002-8591-6231
Rainer Steinbrecher https://orcid.org/0009-0009-8482-9265
Patrick Davies https://orcid.org/0000-0001-9598-4652
Seyni Salack https://orcid.org/0000-0002-1308-6742
Kwame Hackman https://orcid.org/0000-0002-2201-9314

References

Abdul-Ganiyu S, Kyei-Baffour N and Gbedzi V D 2011 Analysis of some hydrological parameters of the Nasia river catchment in the Northern Region of Ghana for its socio-economic development *Afr. J. Agric. Res.* **6** 5533–40 (available at: http://www.academicjournals.org/AJAR)

Addai M O, Yidana S M, Chegbeleh L P, Adomako D and Banoeng-Yakubo B 2016 Groundwater recharge processes in the Nasia sub-catchment of the White Volta Basin: analysis of porewater characteristics in the unsaturated zone *J. Afr. Earth Sci.* **122** 4–14

Akintunde T S, Omolola A P and Oladeji I S 2013 Population dynamics and economic growth in Sub-Saharan Africa *J. Econ. Sustain. Dev.* **4** 147–58 (available at: https://api.semanticscholar.org/CorpusID:54764059)

Alberto M C R, Wassmann R, Buresh R J, Quilty J R, Correa T Q, Sandro J M and Centeno C A R 2014 Measuring methane flux from irrigated rice fields by eddy covariance method using open-path gas analyzer *Field Crops Res.* **160** 12–21

Ali M A, Hoque M A and Kim P J 2013 Mitigating global warming potentials of methane and nitrous oxide gases from rice paddies under different irrigation regimes *Ambio* **42** 357–68

Arouna A, Fatognon I A, Saito K and Futakuchi K 2021 Moving toward rice self-sufficiency in sub-Saharan Africa by 2030: lessons learned from 10 years of the Coalition for African Rice Development *World Dev. Perspect.* **21** 100291

Awuah J 2017 Impact of fire history on carbon storage and vegetation structure in the savanna ecosystem of Mole National Park in the northern region of Ghana *MS Thesis* NTNU

Barthel M *et al* 2022 Low N2O and variable CH4 fluxes from tropical forest soils of the Congo Basin *Nat. Commun.* **13** 330

Berger S *et al* 2019 The impact of rain events on CO2 emissions from contrasting land use systems in semi-arid West African savannas *Sci. Total Environ.* **647** 1478–89

Bin Rahman A N M R and Zhang J 2023 Trends in rice research: 2030 and beyond *Food and Energy Security* vol 12 (John Wiley and Sons Inc.)

Bliefernicht J *et al* 2018 The WASCAL Hydrometeorological Observatory in the Sudan Savanna of Burkina Faso and Ghana *Vadose Zone J.* **17** 1–20

Boucher O, Friedlingstein P, Collins B and Shine K P 2009 The indirect global warming potential and global temperature change potential due to methane oxidation *Environ. Res. Lett.* **4** 044007

Bowell R J and Ansah R K 1994 Mineral status of soils and forage in the Mole National Park, Ghana and implications for wildlife nutrition *Environ. Geochem. Health* **16** 41–58

Breiman L 2001 Random forests *Mach. Learn.* **45** 5–32

Burba G, Madsen R and Feese K 2013 Eddy covariance method for CO2 emission measurements in CCUS applications: principles, instrumentation and software *Energy Proc.* **40** 329–36

Burton A C, Buedi E B, Balangtaa C, Kpelle D G, Sam M K and Brashares J S 2011 The decline of lions in Ghana's Mole National Park *Afr. J. Ecol.* **49** 122–6

Castaldi S, Bertolini T, Nicolini G and Valentini R 2020 Soil is a net source of methane in tropical African forests *Forests* **11** 1–13

Chen Z, Balasus N, Lin H, Nesser H and Jacob D J 2024 African rice cultivation linked to rising methane *Nat. Clim. Change* **14** 148–51

Dakwa K B 2018 Effects of climate and land cover changes on habitat for herbivores at Mole National Park, Ghana *West Afr. J. Appl. Ecol.* **26** 1–13

Dossou-Yovo E R, Devkota K P, Akpoti K, Danvi A, Duku C and Zwart S J 2022 Thirty years of water management research for rice in sub-Saharan Africa: achievement and perspectives *Field Crops Research* vol 283 (Elsevier B.V)

Emerson J B *et al* 2021 Diverse sediment microbiota shape methane emission temperature sensitivity in Arctic lakes *Nat. Commun.* **12**

Fahad S *et al* 2018 Major constraints for global rice production *Advances in Rice Research for Abiotic Stress Tolerance* (Elsevier) pp 1–22

FAO 2021 Emissions from agriculture and forest land. In Global, regional and country trends 1990–2019 (FAO) (available at: www.fao.org/3/cb5293en/cb5293en.pdf)

Feng Z, Wang L, Wan X, Yang J, Peng Q, Liang T, Wang Y, Zhong B and Rinklebe J 2022 Responses of soil greenhouse gas emissions to land use conversion and reversion—A global meta-analysis *Glob. Change Biol.* **28** 6665–78

Foken T and Wichura B 1996 Tools for quality assessment of surface-based flux measurements *Agric. For. Meteorol.* **78** 83–105

Foley J A 2011 Can we feed the world sustain the planet? *Sci. Am.* **305** 60–65

Frankenberg C, Meirink J F, van Weele M, Platt U and Wagner T 2005 Assessing methane emissions from global space-borne observations *Science* **308** 1010–4

Frolking S, Li C, Braswell R and Fuglestvedt J 2004 Short-and long-term greenhouse gas and radiative forcing impacts of changing water management in Asian rice paddies *Glob. Change Biol.* **10** 1180–96

Gasore J 2007 Quantifying emissions of carbon dioxide and methane in central and eastern Africa through high frequency measurements and inverse modeling *MIT* (available at: http://hdl.handle.net/1721.1/115771)

Haque M M, Kim G W, Kim P J and Kim S Y 2016 Comparison of net global warming potential between continuous flooding and midseason drainage in monsoon region paddy during rice cropping *Field Crops Res.* **193** 133–42

Hatala J A, Detto M, Sonnentag O, Deverel S J, Verfaillie J and Baldocchi D D 2012 Greenhouse gas (CO 2, CH 4, H 2O) fluxes from drained and flooded agricultural peatlands in the Sacramento-San Joaquin Delta *Agric. Ecosyst. Environ.* **150** 1–18

Heredia M C, Kant J, Prodhan M A, Dixit S and Wissuwa M 2022 Breeding rice for a changing climate by improving adaptations to water saving technologies *Theoretical and Applied Genetics* vol 135 (Springer Science and Business Media Deutschland GmbH) pp 17–33

IPCC 2014 Climate Change 2014: synthesis Report *Contribution of Working Groups I, II and III to the Fifth Assessment Report of the Intergovernmental Panel on Climate Change* ed

R K Pachauri and L A Meyer (Core Writing Team) (IPCC) p 151
IPCC 2018 Global warming of 1.5 C *An IPCC Special report on the Impacts of Global Warming of 1.5 C Above pre-industrial levels and Related Global Greenhouse Gas Emission Pathways* ed V Masson-Delmotte and P Zhai, *et al* (IPCC)
Irvin J *et al* 2021 Gap-filling eddy covariance methane fluxes: comparison of machine learning model predictions and uncertainties at FLUXNET-CH4 wetlands *Agric. For. Meteorol.* 308–9
James G, Witten D, Hastie T and Tibshirani R 2013 *An Introduction to Statistical Learning* (*Springer Texts in Statistics*) (Springer) (https://doi.org/10.1007/978-1-4614-7138-7)
Jentzsch K, Boike J and Foken T 2021 Importance of the Webb, Pearman, and Leuning (WPL) correction for the measurement of small CO2 fluxes *Atmos. Meas. Tech.* **14** 7291–6
Kaimal J C and Finnigan J J 1994 *Atmospheric Boundary Layer Flows: Their Structure and Measurement* (Oxford university press)
Kim Y, Johnson M S, Knox S H, Black T A, Dalmagro H J, Kang M, Kim J and Baldocchi D 2020 Gap-filling approaches for eddy covariance methane fluxes: a comparison of three machine learning algorithms and a traditional method with principal component analysis *Glob. Change Biol.* **26** 1499–518
Kljun N, Calanca P, Rotach M W and Schmid H P 2015 A simple two-dimensional parameterisation for Flux Footprint Prediction (FFP) *Geosci. Model Dev.* **8** 3695–713
Knox S H *et al* 2021 Identifying dominant environmental predictors of freshwater wetland methane fluxes across diurnal to seasonal time scales *Glob. Change Biol.* **27** 3582–604
Laris P, Koné M, Dembélé F, Rodrigue C M, Yang L, Jacobs R and Laris Q 2021 Methane gas emissions from savanna fires: what analysis of local burning regimes in a working West African landscape tell us *Biogeosciences* **18** 6229–44
Liebethal C and Foken T 2003 On the significance of the webb correction to fluxes *Bound.-Layer Meteorol.* **109** 99–106
Lou Y, Inubushi K, Mizuno T, Hasegawa T, Lin Y, Sakai H, Cheng W and Kobayashi K 2008 CH4 emission with differences in atmospheric CO2 enrichment and rice cultivars in a Japanese paddy soil *Glob. Change Biol.* **14** 2678–87
Lucas-Moffat A M, Schrader F, Herbst M and Brümmer C 2022 Multiple gap-filling for eddy covariance datasets *Agric. For. Meteorol.* **325** 109114
Luo X, Xia T, Huang J, Xiong D and Ridoutt B 2023 Radiative forcing climate footprints in the agricultural sector: comparison of models from the IPCC 5th and 6th Assessment Reports *Farming Syst.* **1** 100057
Maboni C *et al* 2021 The fallow period plays an important role in annual CH4 emission in a rice paddy in Southern Brazil *Sustainability (Switzerland)* **13**
Maier R, Hörtnagl L and Buchmann N 2022 Greenhouse gas fluxes (CO2, N2O and CH4) of pea and maize during two cropping seasons: drivers, budgets, and emission factors for nitrous oxide *Sci. Total Environ.* **849** 157541
Martínez-Eixarch M, Alcaraz C, Viñas M, Noguerol J, Aranda X, Prenafeta-Boldú F X, Català-Forner M, Fennessy M S and Ibáñez C 2021 The main drivers of methane emissions differ in the growing and flooded fallow seasons in Mediterranean rice fields *Plant Soil* **460** 211–27
Mauder M, Cuntz M, Drüe C, Graf A, Rebmann C, Schmid H P, Schmidt M and Steinbrecher R 2013 A strategy for quality and uncertainty assessment of long-term eddy-covariance measurements *Agric. For. Meteorol.* **169** 122–35
Mauder M and Foken T 2006 Impact of post-field data processing on eddy covariance flux estimates and energy balance closure *Meteorol. Z.* **15** 597–609
Mauder M, Foken T, Clement R, Elbers J A, Eugster W, Grünwald T, Grünwald G, Heusinkveld B and Kolle O 2008 Quality control of CarboEurope flux data-Part 2: inter-comparison of eddy-covariance software *Biogeosciences* **5** 451–62
Megonigal J P and Guenther A B 2008 Methane emissions from upland forest soils and vegetation *Tree Physiol.* **28** 491–8
Meijide A, Manca G, Goded I, Magliulo V, Di Tommasi P, Seufert G and Cescatti A 2011 Seasonal trends and environmental controls of methane emissions in a rice paddy field in Northern Italy *Biogeosciences* **8** 3809–21
Ni X and Groffman P M 2018 Declines in methane uptake in forest soils *Proc. Natl Acad. Sci.* **115** 8587–90
Nicholson S E 2013 The West African Sahel: a review of recent studies on the rainfall regime and its interannual variability *ISRN Meteorol.* **2013** 453521
Nikolaisen M, Cornulier T, Hillier J, Smith P, Albanito F and Nayak D 2023a Methane emissions from rice paddies globally: a quantitative statistical review of controlling variables and modelling of emission factors *J. Clean. Prod.* **409** 137245
Nikolaisen M, Hillier J, Smith P and Nayak D 2023b Modelling CH4 emission from rice ecosystem: a comparison between existing empirical models *Front. Agron.* **4**
Nyadzi E, Bessah E, Kranjac-Berisavljevic G and Ludwig F 2021 Hydro-climatic and land use/cover changes in Nasia catchment of the White Volta basin in Ghana *Theor. Appl. Climatol.* **146** 1297–314
O'Connell C S, Ruan L and Silver W L 2018 Drought drives rapid shifts in tropical rainforest soil biogeochemistry and greenhouse gas emissions *Nat. Commun.* **9** 1348–314
Otter L B and Scholes M C 2000 Methane sources and sinks in a periodically flooded South African savanna *Glob. Biogeochem. Cycles* **14** 97–111
Ouyang Z *et al* 2023 Paddy rice methane emissions across Monsoon Asia *Remote Sens. Environ.* 284
Pedregosa F *et al* 2011 Scikit-learn: machine learning in Python *J. Mach. Learn. Res.* **12** 2825–30
Peltola O *et al* 2019 Monthly gridded data product of northern wetland methane emissions based on upscaling eddy covariance observations *Earth Syst. Sci. Data* **11** 1263–89
Potapov P *et al* 2022 Global maps of cropland extent and change show accelerated cropland expansion in the twenty-first century *Nat. Food* **3** 19–28
Quansah E, Mauder M, Balogun A A, Amekudzi L K, Hingerl L, Bliefernicht J and Kunstmann H 2015 Carbon dioxide fluxes from contrasting ecosystems in the Sudanian Savanna in West Africa *Carbon Balance Manage.* **10** 1–17
Rabbi M F and Kovács S 2024 Quantifying global warming potential variations from greenhouse gas emission sources in forest ecosystems *Carbon Res.* **3** 70
Rahman M M and Yamamoto A 2020 Methane cycling in paddy field: a global warming issue *Agrometeorology* (IntechOpen) pp 21
Ramaswamy V *et al* 2001 Radiative forcing of climate change *Climate Change 2001: The Scientific Basis. Contribution of Working Group I to the Third Assessment Report of the Intergovernmental Panel on Climate Change* eds J T Houghton *et al* (Cambridge University Press) pp 350–416
Reba M L, Fong B N, Rijal I, Adviento-Borbe M A, Chiu Y L and Massey J H 2020 Methane flux measurements in rice by static flux chamber and eddy covariance *Agrosyst. Geosci. Environ.* **3** e20119
Saderne V, Dunne A F, Rich W A, Cadiz R, Carvalho S, Cúrdia J and Kattan A 2023 Seasonality of methane and carbon dioxide emissions in tropical seagrass and unvegetated ecosystems *Commun. Earth Environ.* **4** 99
Saito K, Senthilkumar K, Dossou-Yovo E R, Ali I, Johnson J M, Mujawamariya G and Rodenburg J 2023 Status quo and challenges of rice production in sub-Saharan Africa *Plant Production Science* vol 26 (Taylor and Francis Ltd) pp 320–33
Saunois M R *et al* 2020 The global methane budget 2000–2017 *Earth Syst. Sci. Data* **12** 1561–623

Schmitt K and Adu-Nsiah M 1993 *The Vegetation of Mole National Park* (Forest Resource Management Project)

Schotanus P, Nieuwstadt F T M and De Bruin H A R 1983 Temperature measurement with a sonic anemometer and its application to heat and moisture fluxes *Boundary Layer Meteorol.* **26** 81–93

Staudhammer C L, Malone S L, Zhao J, Yu Z, Starr G and Oberbauer S F 2022 Methane emissions from subtropical wetlands: an evaluation of the role of data filtering on annual methane budgets *Agric. For. Meteorol.* **321** 108972

Sulla-Menashe D, Gray J M, Abercrombie S P and Friedl M A 2019 Hierarchical mapping of annual global land cover 2001 to present: the MODIS Collection 6 Land Cover product *Remote Sens. Environ.* **222** 183–94

Swain C K, Bhattacharyya P, Nayak A K, Singh N R, Neogi S, Chatterjee D and Pathak H 2018 Dynamics of net ecosystem methane exchanges on temporal scale in tropical lowland rice *Atmos. Environ.* **191** 291–301

Sy S *et al* 2024 Afforestation in West Africa: potential benefits and trade-offs on regional climate extremes *Preprint* (https://doi.org/10.21203/rs.3.rs-4594282/v1)

Sy S, de Noblet-ducoudré N, Quesada B, Sy I, Dieye A M, Gaye A T and Sultan B 2017 Land-surface characteristics and climate in West Africa: models' biases and impacts of historical anthropogenically-induced deforestation *Sustainability* **9** 1917

United Nations 2016 *World Economic Situation and Prospects* (United Nations publication, Sales No. E.16.II.C.2)

Van Bavel J 2013 The world population explosion: causes, backgrounds and -projections for the future *Facts Views Vis. ObGyn.* **5** 281–91(available at: https://pmc.ncbi.nlm.nih.gov/articles/PMC3987379/)

van der Gaast W, Sikkema R and Vohrer M 2018 The contribution of forest carbon credit projects to addressing the climate change challenge *Clim. Policy* **18** 42–48

van Loon M P, Hijbeek R, ten Berge H F M, De Sy V, ten Broeke G A, Solomon D and van Ittersum M K 2019 Impacts of intensifying or expanding cereal cropping in sub-Saharan Africa on greenhouse gas emissions and food security *Glob. Change Biol.* **25** 3720–30

Vitale D, Fratini G, Bilancia M, Nicolini G, Sabbatini S and Papale D 2020 A robust data cleaning procedure for eddy covariance flux measurements *Biogeosciences* **17** 1367–91

Wang C, Lai D Y F, Sardans J, Wang W, Zeng C and Peñuelas J 2017 Factors related with CH_4 and N_2O emissions from a paddy field: clues for management implications *PLoS ONE* **12** e0169254

Wang H, Li H, Liu Z, Lv J, Song X, Li Q, Jiang H and Peng C 2021 Observed methane uptake and emissions at the ecosystem scale and environmental controls in a subtropical forest *Land* **10** 975

Wanyama I, Pelster D E, Butterbach-Bahl K, Verchot L V, Martius C and Rufino M C 2019 Soil carbon dioxide and methane fluxes from forests and other land use types in an African tropical montane region *Biogeochemistry* **143** 171–90

Weber H and Sciubba J D 2019 The effect of population growth on the environment: evidence from European regions *Eur. J. Popul.* **35** 379–402

Yu L, Huang Y, Zhang W, Li T and Sun W 2017 Methane uptake in global forest and grassland soils from 1981 to 2010 *Sci. Total Environ.* **607** 1163–72

Yuan S, Saito K, van Oort P A J, van Ittersum M K, Peng S and Grassini P 2024 Intensifying rice production to reduce imports and land conversion in Africa *Nat. Commun.* **15** 835

Yvon-Durocher G, Allen A P, Bastviken D, Conrad R, Gudasz C, St-Pierre A, Thanh-Duc N and Del Giorgio P A 2014 Methane fluxes show consistent temperature dependence across microbial to ecosystem scales *Nature* **507** 488–91

Zhang G, Xiao X, Dong J, Xin F, Zhang Y, Qin Y, Doughty R B and Moore B 2020 Fingerprint of rice paddies in spatial–temporal dynamics of atmospheric methane concentration in monsoon Asia *Nat. Commun.* **11** 554

Zhao J F *et al* 2019 Tropical forest soils serve as substantial and persistent methane sinks *Sci. Rep.* **9** 16799

Zhu D *et al* 2021 Methane emissions respond to soil temperature in convergent patterns but divergent sensitivities across wetlands along altitude *Glob. Change Biol.* **27** 941–55

Zhu S, McCalmont J, Cardenas L M, Cunliffe A M, Olde L, Signori-Müller C, Litvak M E and Hill T 2023 Gap-filling carbon dioxide, water, energy, and methane fluxes in challenging ecosystems: comparing between methods, drivers, and gap-lengths *Agric. For. Meteorol.* **332** 109365